Rapid Communications

Anomalous linear magnetoresistance in high-quality crystalline lead thin films

Yi Liu,[1,2] Yue Tang,[1,2] Ziqiao Wang,[1,2] Chaofei Liu,[1,2] Cheng Chen,[1,2] and Jian Wang[1,2,3,4,*]

[1]*International Center for Quantum Materials, School of Physics, Peking University, Beijing 100871, China*

[2]*Collaborative Innovation Center of Quantum Matter, Beijing 100871, China*

[3]*CAS Center for Excellence in Topological Quantum Computation, University of Chinese Academy of Sciences, Beijing 1001090, China*

[4]*Beijing Academy of Quantum Information Sciences, Beijing 100193, China*

(Received 13 January 2020; accepted 15 September 2020; published 7 October 2020)

Intriguing novel phenomena in lead films have inspired a new understanding of quantum physics, such as the quantum size effect and quantum phase transitions, etc. The improvement of the sample quality makes it even more promising to explore the intrinsic properties in two-dimensional systems. In this Rapid Communication, we show that the crystalline interfacial striped incommensurate layer can increase the quality of the lead films and significantly enhance the magnitude of magnetoresistance. By performing systematic transport measurements, a predominant anomalous linear magnetoresistance is revealed, and the widely used Parish-Littlewood model and Abrikosov's explanation fail to describe the observation. Instead, we propose another model of linear magnetoresistance based on linear band structure, which shows good agreement with the experimental results. Our studies reveal a different origin of linear magnetoresistance which may also be helpful to understand the linear magnetoresistance in other materials with a linear dispersion of the electronic structure.

DOI: 10.1103/PhysRevB.102.140403

Crystalline lead films have been investigated over the past 30 years and have gained growing interest since intriguing phenomena [e.g., the quantum size effect [1], superconductivity in the two-dimensional (2D) limit [2–4]] are being continuously discovered, which have significantly deepened our understanding of low-dimensional physics [5–10]. One problem influencing the quality of crystalline lead films is the lattice mismatch between the films and the substrate. This mismatch, which results in an amorphous interface (called the wetting layer), makes it difficult to prepare atomically uniform ultrathin films [11], leading to a relatively low mobility and a small magnetoresistance (MR) of films. One solution to this mismatch is to grow a crystalline reconstruction phase as the interface between Pb films and the Si substrate, such as the striped incommensurate (SIC) phase, $\sqrt{7} \times \sqrt{3}$ phase, etc. Consequently, several novel phenomena have been observed in ultrathin lead films including interface-induced Ising superconductivity [12], anomalous quantum Griffith singularity [13], and so on. These findings well manifest the abundant physical mechanisms concealed in ultrathin crystalline lead films and inspire continuous enthusiasm for investigations on low-dimensional crystalline systems.

The MR measurement is a typical and useful method to reveal the physical properties including the density of states (DOS), mobility, and band structures. One striking phenomenon is linear magnetoresistance (LMR), which could be observed in some special situations and may survive up to a very high magnetic field [14–16] (e.g., LMR in a Cd_3As_2 crystal can survive up to 60 T). In theory, the Parish-Littlewood (PL) model [17] and Abrikosov's quantum explanation [18,19] are widely used to describe the LMR. The classical PL model attributes the LMR in disordered systems to a large inhomogeneity, which distorts the current flow and introduces transverse Hall resistance to longitudinal conducting compositions. Another mechanism of LMR was found by Abrikosov, who ascribed LMR to the intrinsic quantum states of systems. If the system reaches an "extreme quantum limit," which means that the electrons all stay at the first Landau level, the LMR would appear naturally according to Abrikosov's quantum explanation [18]. However, not all cases could be well explained by these two models such as the LMR in iron-based superconductors [20], Dirac semimetals [21], and ferromagnetic semiconductors [22]. Several novel mechanisms have been proposed, including spin fluctuation and the d band shift [22]. In order to reach a deeper and wider understanding of LMR in various systems, further experiments and explanations are highly desired.

In this Rapid Communication, we report transport measurements on 10-monolayer (ML) and 20-ML crystalline lead films grown on the SIC phase on a Si(111) substrate via molecular beam epitaxy (MBE). Compared to a lead film grown on amorphous wetting layers, the 20-ML Pb film grown on the SIC layer exhibits significantly larger mobility. As a result, a large enhancement of MR is observed in this system. To be specific, under a perpendicular magnetic field, the MR, defined as $\mathrm{MR} = [R(H) - R(0)]/R(0)$, reaches 3% and 11% under 15 T at 10 K in 10- and 20-ML Pb films with a SIC phase interface. Pb thin films follow the classical quadratic field dependence in low magnetic field regimes, however, a predominant LMR appears at 5 T and exists up to 15 T. The widely used PL model and Abrikosov's explanation fail to explain our observations. We ascribe the detected LMR in 2D

*Corresponding author: jianwangphysics@pku.edu.cn

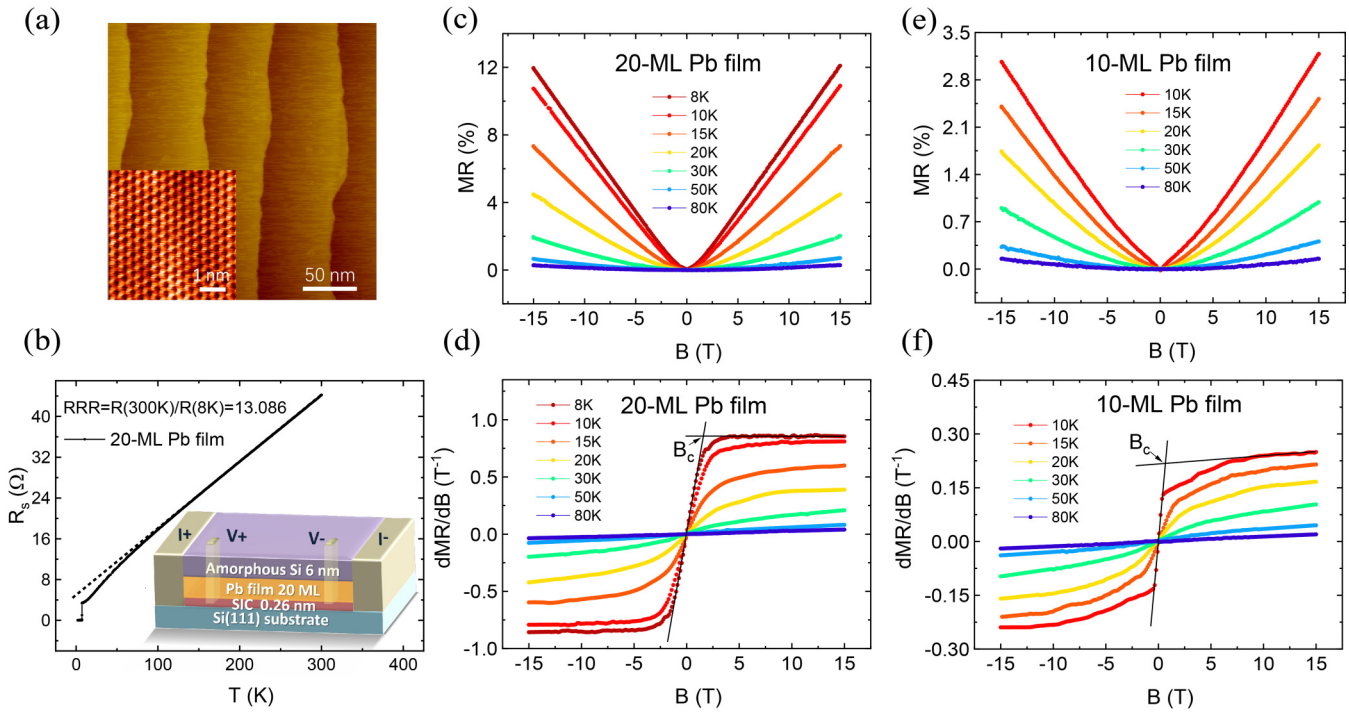

FIG. 1. Morphology and transport properties of Pb thin films. (a) A typical STM image of 20-ML Pb film (250 nm × 250 nm). Inset: Atomically resolved STM image of 20-ML Pb film (5nm × 5nm). (b) Temperature dependence of sheet resistance on 20-ML Pb film at zero magnetic field, showing RRR of 13.086 defined as the ratio of resistance at 300 and 8 K [RRR = $R(300K)/R(8K)$]. The inset is a schematic diagram for standard four-electrode transport measurements. Perpendicular magnetic field dependence of sheet resistance for (c) 20-ML and (d) 10-ML Pb films on a SIC phase interface. The corresponding derivative MR (dMR/dB) is shown in (e) and (f), respectively.

films to the changes in the DOS for linear bands at the Fermi surface.

Figure 1(a) presents the morphology and atomically resolved image of a 20-ML lead film measured by scanning tunneling microscopy (STM), indicating the high quality of samples grown on the SIC phase. The transport properties at zero magnetic field of a 20-ML Pb film are shown in Fig. 1(b). A relatively large residual resistance ratio (RRR) of 13 [defined as the ratio of resistance at 300 and 8 K, RRR = R(300 K)/R(8 K)] is observed, which is twice as large as that of the samples grown on amorphous wetting layers (Fig. S2 [23]), showing the great improvement in sample quality by using the SIC phase interface. The schematic of the standard four-electrode transport measurement is presented in the inset of Fig. 1(b). Figures 1(c) and 1(d) summarize the perpendicular field dependence of longitudinal resistance for both 10- and 20-ML lead films at various temperatures. The MR monotonically decreases with increasing temperature, which can be ascribed to the decreasing mobility at higher temperatures (Fig. S3 [23]). Under a low magnetic field, MR increases quadratically, and, strikingly, as the field exceeds 5 T, MR gradually turns to a linear behavior. The change from parabolic MR to LMR could be shown more clearly in the field-dependent dMR/dB [Figs. 1(e) and 1(f)]. The intercept of the dMR/dB vs B curve represents the linear terms (MR $\propto B$) while the gradient refers to the quadratic component (MR $\propto B^2$) (see Eq. (1)). The intercepts of the curves in the high-field regime remain finite below 30 K, indicating the survival of LMR. The LMR at relatively low temperatures (a large intercept and small slope) gradually evolves to quadratic behavior (a small intercept and large slope) at higher temperatures, revealing the appearance of a parabolic term and the disappearance of LMR with increasing temperatures. In Figs. 1(e) and 1(f), the curves could be separated into three different parts. The first part is a straight line passing the origin at low fields (quadratic term), the second is a smooth transition region, and the last is a straight line with a reduced gradient (linear and quadratic terms). The MR in the first and the last parts could be expressed as [37]

$$\frac{d\mathrm{MR}}{dB} = \begin{cases} 2A_0\mu^2 B, & B < B_c, \\ A_1\mu + 2A_2\mu^2 B, & B \geqslant B_c, \end{cases} \tag{1}$$

$$\mathrm{MR} = \begin{cases} A_0\mu^2 B^2, & B < B_c, \\ A_1\mu B + A_2\mu^2 B^2, & B \geqslant B_c, \end{cases} \tag{2}$$

where A_0, A_1, and A_2 are constant parameters, μ is the mobility, and the crossover field B_c corresponds to the crossing point of two black solid lines. Equation (2) includes the parabolic term of MR with the coefficient A_0 under low field and a linear component plus a quadratic term with the coefficients A_1 and A_2 at high fields, respectively. As shown in Fig. 2, the values of A_0 and A_1 generally decreases and A_2 increases with increasing temperature. The increasing A_2 is quite distinct from the previous study showing a decreasing coefficient of the quadratic term when the temperature is increasing [37]. In the Pb films, A_2 (the quadratic term in the high-field region) increases with increasing temperature and is finally almost equal to A_0 (the quadratic term in the low-field region), indicating the disappearance of LMR.

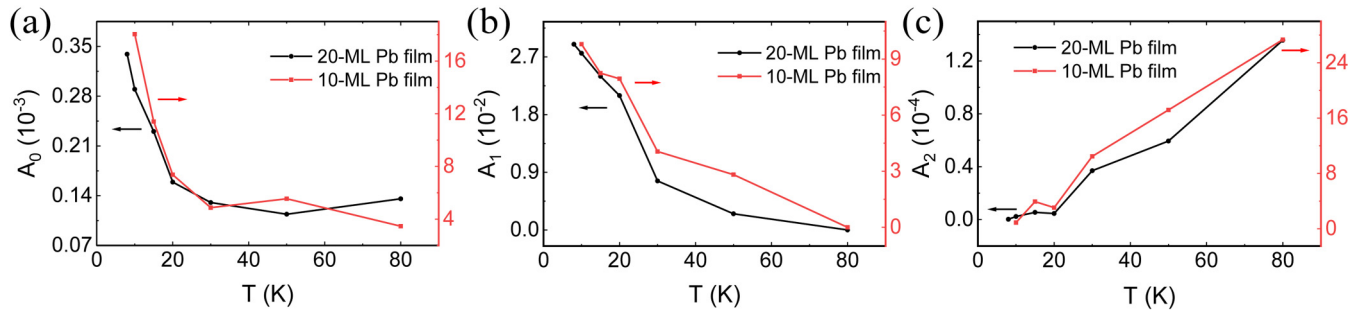

FIG. 2. Temperature dependence of the (a) low-field quadratic term coefficient A_0, (b) high-field linear term coefficient A_1, and (c) high-field quadratic term coefficient A_2 for 10- and 20-ML Pb films. All the coefficients are obtained from the fitting results of Eq. (2).

Figure 3 shows the temperature dependence of the crossover field extracted from Fig. 1(e) and 1(f) for both 20- and 10-ML Pb films (see Fig. S11 for the extraction of B_c above 30 K for the 20-ML Pb film [23]). The crossover field monotonically increases with increasing temperature and shows a tendency for saturation around 50 K. As shown in Fig. 3, the crossover field could be well fitted by a thermal activation equation (the red lines in Fig. 3) which reads $B_c = Ae^{-\frac{\Delta}{k_B T}} + C$, where Δ is the activation energy, A and C are coefficients, and k_B is the Boltzmann constant. The relatively large DOS in the Pb films makes the quantum limit much larger than 15 T, thus Abrikosov's quantum scenario is not consistent with our observation [23]. The classical PL model predicts that LMR more likely occurs in a more disordered system, however, the 20-ML Pb film with relatively high mobility exhibits a clearer LMR compared to the 10-ML Pb film with low mobility. Besides, the behaviors of $1/\mu$ vs B_c curves are found to contradict the expectation of the PL model [23]. Moreover, the theories based on the orbital effects and the scattering of the cyclotron electrons including the "hot spot" theory [30–32] can also be excluded due to the observation of LMR under a parallel field (detailed discussions are given in the Supplemental Material [23]).

To understand the observed LMR, we propose a phenomenological model based on the linear band structure. In our model, we assume a small region of a Dirac-type band (linear dispersion) around the Fermi surface and the other bands are the normal parabolic bands resulting in the quadratic behavior of MR. Figure 4(a) presents the DOS versus energy of the aforementioned band structure. In 2D systems, the DOS $N(E)$ of the parabolic band is independent of energy [the vertical solid line in Fig. 4(a)] while the $N(E)$ of the Dirac-type band linearly changes with increasing energy values [the solid line with a finite slope in Fig. 4(a)]. The up and down arrows on the x axis represent the two opposite directions of spins and the y axis separates the band structure with different spin directions. The blue area represents the occupied electron states and the band structure takes a hole-type shape since holes are predominant in lead films. When an external magnetic field is increasing, Zeeman splitting would lead to the opposite shift of the band structures and the electrons in the elevated bands would naturally tend to lower their energy and thus jump to the states with opposite spin directions [illustrated by the curved arrow in Fig. 4(a)]. In Fig. 4(a), the spin splitting is linear to the external magnetic field ($\delta h = g\mu_B B$, where g is the Landé factor and μ_B is the Born magneton), and leads to the slight increase of the Fermi level (black dashed line).

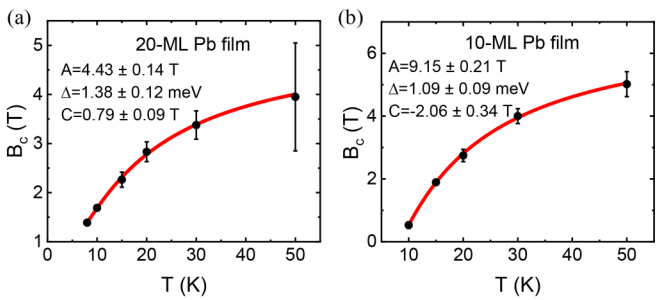

FIG. 3. Temperature dependence of the crossover field B_c for both (a) 20-ML and (b) 10-ML films. The red lines are theoretical fitting curves ($B_c = Ae^{-\frac{\Delta}{k_B T}} + C$). The fitting parameters $A, C,$ and Δ are summarized in this figure.

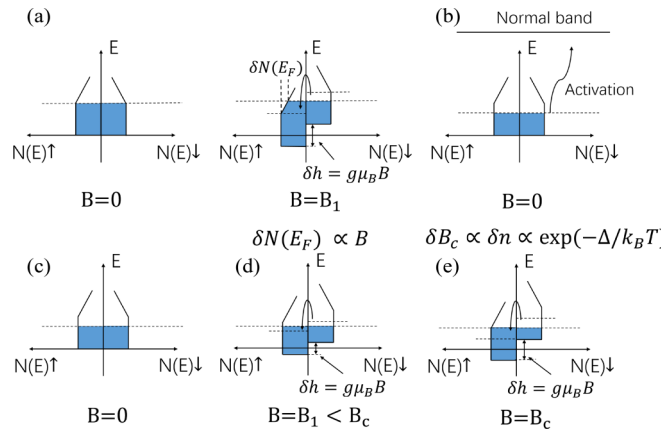

FIG. 4. Illustrations for the origin of LMR. (a) The DOS dependence of energy in the band structure consisting of linear (the oblique lines) and quadratic bands (the vertical lines) in a 2D system. The blue color represents the states occupied by electrons and the horizontal dashed line represents the Fermi surface while the vertical dashed lines represent the change of DOS, $\delta N(E_F)$, at the Fermi level. The change of DOS at the Fermi surface leads to LMR. (b) Illustration of the thermally activated behavior of crossover field. (c)–(e) Illustration of the appearance of LMR. Only when the magnetic field makes the Fermi surface reach the border of linear bands does the DOS start a relatively large change leading to the appearance of LMR.

Thus, the DOS in the Fermi level also decreases [marked as $\delta N(E_F)$] and consequently affects the value of the conductance. The change in DOS is proportional to the magnetic field $\delta N(E_F) = -\gamma g \mu_B B$, where γ is a constant determined by the shape of the band structures. In 2D systems the conductance can be expressed as $\sigma = \frac{1}{2} j_F^2 \tau(E_F) N(E_F)$ [23]. Thus, the MR can be deduced as

$$\frac{\delta\rho(B)}{\rho_0} = -\frac{\delta\sigma(B)}{\sigma_0} = -\frac{\delta(\tau(E_F)N(E_F))}{\tau_0 N_0} = -\frac{\tau(E_F)\delta N(E_F)}{\tau_0 N_0} + \tau(E_F)\delta\left(\frac{1}{\tau}\right)\frac{N(E_F)}{N_0}, \tag{3}$$

where j_F is a constant representing the Fermi-surface current density and τ is the relaxation rate. The Pb film is a typical s-wave superconductor where the electron-phonon interaction is dominant. Therefore, the relaxation rate of Pb thin films can be understood by the deformation potential theory [33,34] and thus can be expressed as $\frac{1}{\tau} = \frac{1}{\tau_0} + \frac{1}{\tau_{de}} = \frac{1}{\tau_0} + K(T)N(E)$ [33,34,38,39], where τ_0 is the term independent of the magnetic field and $K(T)$ is a temperature-dependent function. After applying this function in Eq. (3), the LMR can be deduced clearly,

$$\mathrm{MR} = \frac{\delta\rho(B)}{\rho_0} = -\frac{\delta N(E_F)}{N_0}\left(\frac{1}{1+KN_0\tau_0}\right)^2 \propto \frac{B}{N_0\cdot(1+KN_0\tau_0)^2}. \tag{4}$$

Interestingly, the crossover from the low-field quadratic MR to high-field LMR can also be explained in the framework of our phenomenological model. In Fig. 4(c), the Fermi surface is initially in the quadratic band area. When the external field slightly shifts the DOS of the bands (corresponding to the small magnetic field regime) and the electrons have not reached the linear band regime, the DOS at the Fermi surface remains a constant and cannot give rise to the LMR [Fig. 4(d)]. Only when the field is large enough to make the electron occupy the states in the linear band, does the DOS begin to decrease and lead to the LMR [Fig. 4(e)]. The field required to reach the border of the linear bands is the crossover field B_c. Furthermore, the observed thermally activated behavior of B_c (Fig. 3) can be understood as follows. At finite temperatures, the thermal activation would bring some of the lower band's electrons to the upper band [Fig. 4(b)]. The number of such electrons shows an activation function relationship with the temperature $\delta n \propto \exp(-\frac{\Delta}{k_B T})$, where Δ describes the gap between the lower and upper bands. Since the number of electrons decreases at lower bands, a higher magnetic field is required to make the lower band's electron reach the border of linear bands. Therefore, the crossover field also shows a thermal activation behavior. Indeed, the data in Fig. 3 can be well fitted by the thermal activation function $B_c = Ae^{-\frac{\Delta}{k_B T}} + C$ with an activation energy of 1.4 and 1.0 meV for the 20- and 10-ML Pb films, respectively. The small activation energy could exist in the lead thin films due to the intricate band structures [12]. Moreover, the Kohler rule cannot be applied to our systems (Fig. S6 [23]). The inapplicability of the Kohler rule is consistent with the proposed model since our model assumes a scattering time dependent on the external magnetic field.

The expectations of our model are well consistent with the experimental data. The main assumption of this model is the existence of a linear band in a small region near the Fermi level, which has been indicated by previous works, including band-structure calculations and angle-resolved photoemission spectroscopy (ARPES) measurements. The ARPES data of 21-ML Pb films along the ΓM direction show linear bands away from the Γ point and parabolic bands around the Γ point, which is confirmed by the band-structure calculations [40]. Further investigations on 23- and 24-ML Pb films along the ΓK direction reveal similar band structures with linear energy dispersion near the Fermi surface [41]. The emergence of linear bands near the Fermi level is also widely observed in thinner films, such as 6- to 10-ML Pb films [42–45]. Therefore, the band structure of Pb thin films exhibits both parabolic and linear bands, which is well consistent with our model. Moreover, the prevailing classical PL model explains the LMR in disordered systems [17,25,46], while Abrikosov's quantum explanation requires the quantum limit [18], which is very hard to reach for most materials. Different from them, our work proposes another model of LMR, which is not only a different understanding of LMR, but also inspires further investigations on the linear MR in 2D systems with a linear energy dispersion (e.g., the topological materials and high-temperature superconductors FeSe and $FeTe_{1-x}Se_x$, etc.), especially for those with less disorder and a relatively high carrier density.

In summary, with the improvement of sample quality, we performed detailed magnetic transport measurements on both 10- and 20-ML crystalline Pb films. Surprisingly, a pronounced LMR is detected from 8 to 30 K in both films and cannot be interpreted by the widely accepted theories, i.e., the classical PL model and Abrikosov's quantum explanation. With an attempt to understand the concealing mechanism of the observed LMR, we propose a phenomenological model based on a band structure composed of linear and quadratic bands, which suggests that the observed LMR originates from the changes of DOS at the Fermi surface. The model can well describe the crossover from quadratic MR to LMR and explains the temperature dependence of B_c. With systematic studies of MR in Pb thin films, our work reveals a different mechanism of LMR, which could be applied to various 2D materials with linear energy dispersion.

We thank Professor Haiwen Liu for a fruitful discussion and Professor Ying Xing for help with the transport measurement. This work was financially supported by the National Key Research and Development Program of China (Grants No. 2018YFA0305604 and No. 2017YFA0303302), the National Natural Science Foundation of China (Grants No. 11888101 and No. 11774008), the Strategic Priority Research Program of the Chinese Academy of Sciences (Grant No. XDB28000000), Beijing Natural Science Foundation (Z180010), and China Postdoctoral Science Foundation (Grants No. 2019M650290 and No. 2020T130021).

Y.L. and Y.T. contributed equally to this work.

[1] Y. Guo, Y.-F. Zhang, X.-Y. Bao, T.-Z. Han, Z. Tang, L.-X. Zhang, W.-G. Zhu, E. G. Wang, Q. Niu, Z. Q. Qiu, J.-F. Jia, Z.-X. Zhao, and Q.-K. Xue, Science **306**, 1915 (2004).

[2] T. Zhang, P. Cheng, W.-J. Li, Y.-J. Sun, G. Wang, X.-G. Zhu, K. He, L. Wang, X. Ma, X. Chen, Y. Wang, Y. Liu, H.-Q. Lin, J.-F. Jia, and Q.-K. Xue, Nat. Phys. **6**, 104 (2010).

[3] S. Qin, J. Kim, Q. Niu, and C.-K. Shih, Science **324**, 1314 (2009).

[4] M. Yamada, T. Hirahara, and S. Hasegawa, Phys. Rev. Lett. **110**, 237001 (2013).

[5] H. H. Weitering, D. R. Heslinga, and T. Hibma, Phys. Rev. B **45**, 5991 (1992).

[6] M. M. Özer, J. R. Thompson, and H. H. Weitering, Nat. Phys. **2**, 173 (2006).

[7] D. Eom, S. Qin, M. Y. Chou, and C. K. Shih, Phys. Rev. Lett. **96**, 027005 (2006).

[8] C. Brun, T. Cren, V. Cherkez, F. Debontridder, S. Pons, D. Fokin, M. C. Tringides, S. Bozhko, L. B. Ioffe, B. L. Altshuler, and D. Roditchev, Nat. Phys. **10**, 444 (2014).

[9] Y. Saito, T. Nojima, and Y. Iwasa, Nat. Rev. Mater. **2**, 16094 (2016).

[10] C. Brun, I.-P. Hong, F. Patthey, I. Y. Sklyadneva, R. Heid, P. M. Echenique, K. P. Bohnen, E. V. Chulkov, and W.-D. Schneider, Phys. Rev. Lett. **102**, 207002 (2009).

[11] Y.-F. Zhang, J.-F. Jia, Z. Tang, T.-Z. Han, X.-C. Ma, and Q.-K. Xue, Surf. Sci. **596**, L331 (2005).

[12] Y. Liu, Z. Wang, X. Zhang, C. Liu, Y. Liu, Z. Zhou, J. Wang, Q. Wang, Y. Liu, C. Xi, M. Tian, H. Liu, J. Feng, X. C. Xie, and J. Wang, Phys. Rev. X **8**, 021002 (2018).

[13] Y. Liu, Z. Wang, P. Shan, Y. Tang, C. Liu, C. Chen, Y. Xing, Q. Wang, H. Liu, X. Lin, X. C. Xie, and J. Wang, Nat. Commun. **10**, 3633 (2019).

[14] Y. Zhao, H. Liu, C. Zhang, H. Wang, J. Wang, Z. Lin, Y. Xing, H. Lu, J. Liu, Y. Wang, S. M. Brombosz, Z. Xiao, S. Jia, X. C. Xie, and J. Wang, Phys. Rev. X **5**, 031037 (2015).

[15] T. Khouri, U. Zeitler, C. Reichl, W. Wegscheider, N. E. Hussey, S. Wiedmann, and J. C. Maan, Phys. Rev. Lett. **117**, 256601 (2016).

[16] X. Zhang, T. Luo, X. Hu, J. Guo, G. Lin, Y. Li, Y. Liu, X. Li, J. Ge, Y. Xing, Z. Zhu, P. Gao, L. Sun, and J. Wang, Chin. Phys. Lett. **36**, 057402 (2019).

[17] M. M. Parish and P. B. Littlewood, Nature (London) **426**, 162 (2003).

[18] A. A. Abrikosov, Phys. Rev. B **58**, 2788 (1998).

[19] A. A. Abrikosov, Europhys. Lett. **49**, 789 (2000).

[20] Q. Wang, W. Zhang, W. Chen, Y. Xing, Y. Sun, Z. Wang, J.-W. Mei, Z. Wang, L. Wang, X.-C. Ma, F. Liu, Q.-K. Xue, and J. Wang, 2D Mater. **4**, 034004 (2017).

[21] M. Novak, S. Sasaki, K. Segawa, and Y. Ando, Phys. Rev. B **91**, 041203(R) (2015).

[22] K. J. Kormondy, L. Gao, X. Li, S. Lu, A. B. Posadas, S. Shen, M. Tsoi, M. R. McCartney, D. J. Smith, J. Zhou, L. L. Lev, M.-A. Husanu, V. N. Strocov, and A. A. Demkov, Sci. Rep. **8**, 7721 (2018).

[23] See Supplemental Material at http://link.aps.org/supplemental/10.1103/PhysRevB.102.140403 for details, which also includes Refs. [24–36].

[24] J. Hu and T. F. Rosenbaum, Nat. Mater. **7**, 697 (2008).

[25] Z. H. Wang, L. Yang, X. J. Li, X. T. Zhao, H. L. Wang, Z. D. Zhang, and X. P. A. Gao, Nano Lett. **14**, 6510 (2014).

[26] A. L. Friedman, J. L. Tedesco, P. M. Campbell, J. C. Culbertson, E. Aifer, F. K. Perkins, R. L. Myers-Ward, J. K. Hite, C. R. Eddy, G. G. Jernigan, and D. K. Gaskill, Nano Lett. **10**, 3962 (2010).

[27] W. Wang, Y. Du, G. Xu, X. Zhang, E. Liu, Z. Liu, Y. Shi, J. Chen, G. Wu, and X.-x. Zhang, Sci. Rep. **3**, 2181 (2013).

[28] J. M. Ziman, *Electrons and Phonons* (Oxford University Press, Oxford, UK, 1960).

[29] D. Shoenberg, *Magnetic Oscillation in Metals* (Cambridge University Press, Cambridge, UK, 1984).

[30] A. A. Sinchenko, P. D. Grigoriev, P. Lejay, and P. Monceau, Phys. Rev. B **96**, 245129 (2017).

[31] Y. Feng, Y. Wang, D. M. Silevitch, J. Q. Yan, R. Kobayashi, M. Hedo, T. Nakama, Y. Ōnuki, A. V. Suslov, B. Mihaila, P. B. Littlewood, and T. F. Rosenbaum, Proc. Natl. Acad. Sci. U.S.A. **116**, 11201 (2019).

[32] B. Wu, V. Barrena, F. Mompeán, M. García-Hernández, H. Suderow, and I. Guillamón, Phys. Rev. B **101**, 205123 (2020).

[33] J. M. Ziman, *Principles of the Theory of Solids* (Cambridge University Press, Cambridge, UK, 1972).

[34] J. Bardeen and W. Shockley, Phys. Rev. **80**, 72 (1950).

[35] A. E. Dolbak, R. A. Zhachuk, and B. Z. Olshanetsky, Cent. Eur. J. Phys. **2**, 254 (2004).

[36] R. P. Elliott, *Constitution of Binary Alloys, First Supplement* (McGraw-Hill, New York, 1965).

[37] Y. Sun, S. Pyon, and T. Tamegai, Phys. Rev. B **93**, 104502 (2016).

[38] M. T. Dylla, S. D. Kang, and G. J. Snyder, Angew. Chem., Int. Ed. **58**, 5503 (2019).

[39] H. Goldsmid, *Thermoelectric Refrigeration* (Springer, Berlin, 2013).

[40] S. He, Z. Zeng, M. Arita, M. Sawada, K. Shimada, S. Qiao, G. Li, W.-X. Li, Y.-F. Zhang, Y. Zhang, X. Ma, J. Jia, Q.-K. Xue, H. Namatame, and M. Taniguchi, New J. Phys. **12**, 113034 (2010).

[41] Y. J. Sun, S. Souma, W. J. Li, T. Sato, X. G. Zhu, G. Wang, X. Chen, X. C. Ma, Q. K. Xue, J. F. Jia, T. Takahashi, and T. Sakurai, Nano Res. **3**, 800 (2010).

[42] J. H. Dil, J. W. Kim, T. Kampen, K. Horn, and A. R. H. F. Ettema, Phys. Rev. B **73**, 161308(R) (2006).

[43] N. Miyata, K. Horikoshi, T. Hirahara, S. Hasegawa, C. M. Wei, and I. Matsuda, Phys. Rev. B **78**, 245405 (2008).

[44] J. H. Dil, F. Meier, J. Lobo-Checa, L. Patthey, G. Bihlmayer, and J. Osterwalder, Phys. Rev. Lett. **101**, 266802 (2008).

[45] M. Müller, N. Néel, S. Crampin, and J. Kröger, Phys. Rev. B **96**, 205426 (2017).

[46] R. Xu, A. Husmann, T. F. Rosenbaum, M. L. Saboungi, J. E. Enderby, and P. B. Littlewood, Nature (London) **390**, 57 (1997).